Highly efficient and stable photocatalytic CO_2 and H_2O reduction into methanol at lower temperatures through an elaborate gas-liquid-solid interfacial system

Haitao Yu [a], Yimin Xuan[*] [a, b], Qibin Zhu [a, b], Sheng Chang [a]

[a] School of Energy and Power Engineering, Nanjing University of Aeronautics and Astronautics, Nanjing 210001, China.

[b] Key Laboratory of Thermal Management and Energy Utilization of Aviation Vehicles, Ministry of Industry and Information Technology.

[*] Corresponding authors

Prof. Y. Xuan

E-mail: ymxuan@nuaa.edu.cn

[a] School of Energy and Power Engineering, Nanjing University of Aeronautics and Astronautics, Nanjing 210001, China.

Experimental

Preparation of $SrTiO_3$ (La, Cr):

4.0507g titanium isopropoxide (Aladdin Industrial Corporation; 99.9%) is dissolved in 33.5ml glycol (Shanghai Macklin Biochemical Co. Ltd.; 98%). Then 31.521g of citric acid (Chronchemicals; 99%) is added to the mixture. The mixture is stirred vigorously at 50 ° C until it became transparent. 4.1461g strontium acetate (Aladdin Industrial Corporation; 99.9%), 0.3248 g $La(NO_3)_3 \cdot 6H_2O$ (Nanjing Reagent; 99%), and 0.3001 g $Cr(NO_3)_3 \bullet 9H_2O$ (Nanjing Reagent; 99%) were added to the mixture and further stirred at 50℃ for 4 h to yield a completely dissolved reaction mixture. The solution was pyrolyzed at 350 ℃ for 2 h. The resulting black solid product was crushed with an agate mortar, then the powder was calcined at

900℃ for 2 h in the air at a temperature-programmed Muffle furnace. The yellow solid was produced and soaked in 1M/L dilute hydrochloric acid for 24 hours. The solid was washed with water and dried at 95℃ for 24 h. The resultant product was ball milled for half an hour at a speed of 400 r/min.

Materials characterization

The XRD analyses of different simples were performed using Bruker D8 Advance X-ray diffractometer with Cu-Kα radiation (λ = 0.154178 nm) at 40 kV and 40 mA. TEM images and HRTEM images were taken on Talos f200x, America. And the acceleration voltage is 200kV. The prepared particles are sonicated in ethanol for 30 minutes before TEM analysis. The morphology of composite particles is examined by Field Emission Scanning Electron Microscope (SEM) (Zeiss Gemini sem300, Germany). And the acceleration voltage Is 5 kV. To study the distribution of elements, element mapping Is carried out for different materials. And the content and concentration of elements in each material are tested by Energy Dispersive X-ray spectroscopy (EDS) (Talos f200x, America). X-ray photoelectron spectroscopy (XPS) analysis (Thermo Fisher k-alpha, America) is used to examine the effects of hydrogenation on chemical composition and oxidation state. UV-Vis-NIR spectral (Lambda 1050+, America) of different photocatalysts is also carried out. Photoluminescence (PL) spectra of the photocatalyst powders are recorded using a Steady-state/Transient Fluorescence spectrometer (1000, Edinburgh) and all test conditions remained the same. GC 9720plus (GC, Zhejiang Fuli Analytical Instrument Co., Ltd.) equipped with a thermal conductivity detector (TCD) and flame ionization detector (FID) is used to analyze gaseous products. Gas chromatography-mass spectroscopy (Agilent, 5977b) was used to prove that the reduction product methanol was directly derived from $^{13}CO_2$. Temperature programmed desorption of CO_2 by Micromeritics AutoChem II 2920. The 0.192 g of catalyst is treated with He at 300 ° C for 1 hour and then cooled to 20 ° C. Then CO_2 was continued to pass in for 1 h. The sample is then flushed with the gas of He

to eliminate any physically adsorbed CO_2. The desorption peak is noted while the temperature is varied by 10 °C/min. To study the distribution of elements, element mapping and mapping are carried out for different materials.

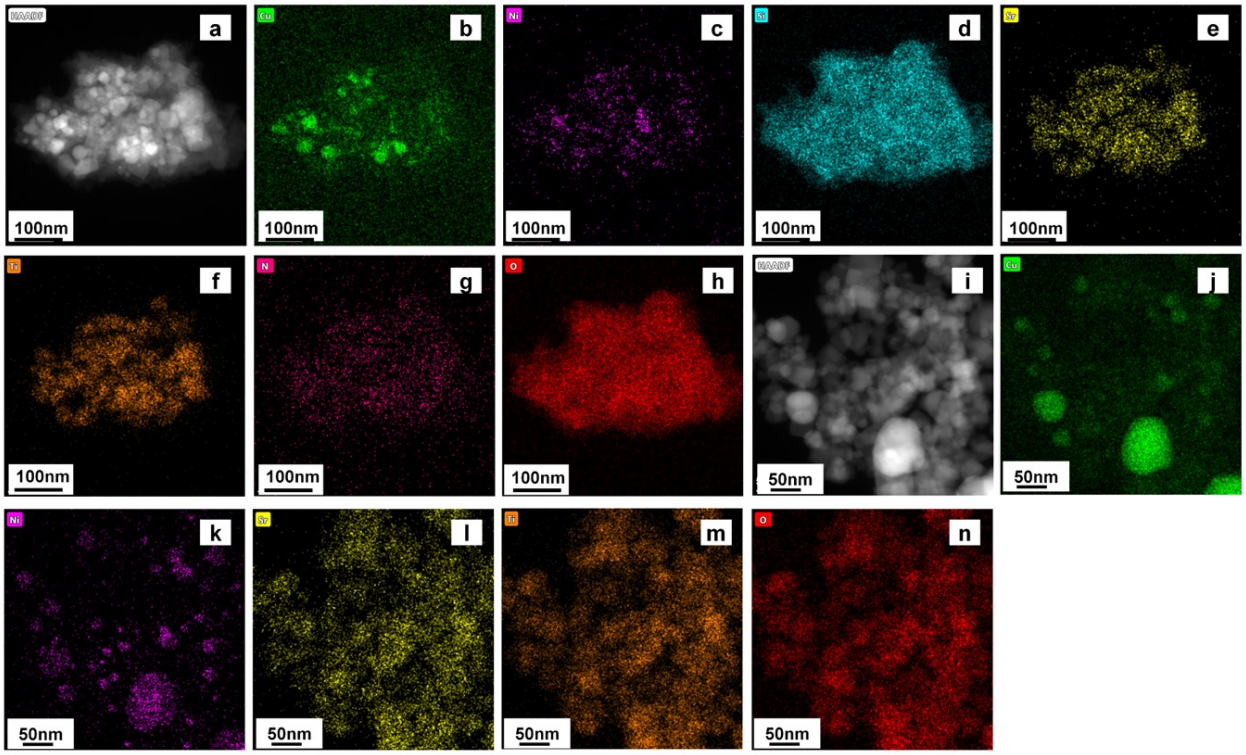

Fig. S1 (a)-(h) the elemental mapping images of Cu, Ni, Si, Sr, Ti, N, and O of STO/Cu@Ni/SiO_2/TiN, (i)-(n) the elemental mapping images of Cu, Ni, Sr, Ti, and O of STO/Cu@Ni

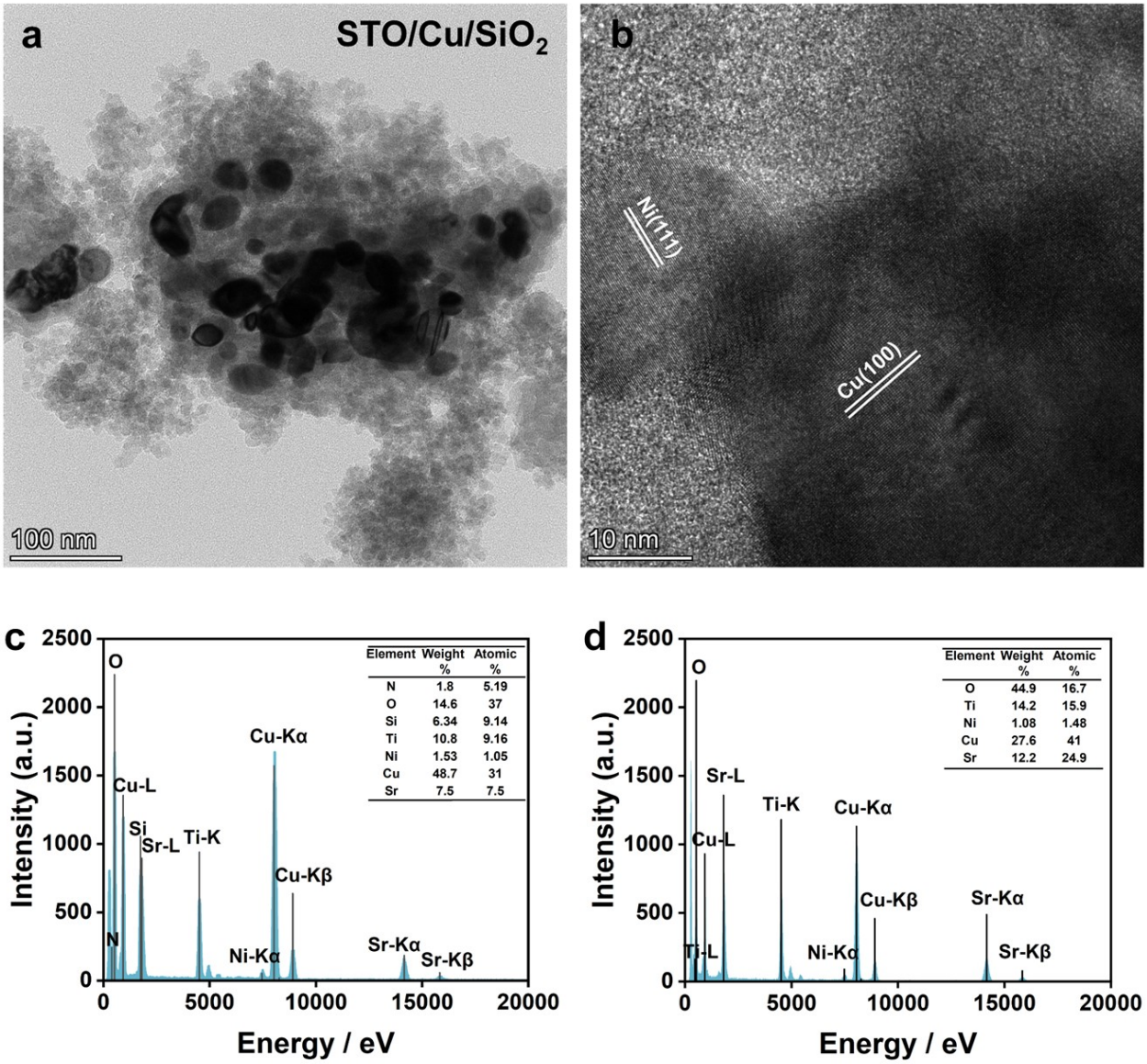

Fig. S2 (a) the TEM image of STO/Cu/SiO_2, (b) the HRTEM image of STO/Cu@Ni/SiO_2/TiN, (c) the EDX spectrum of STO/Cu@Ni/SiO_2/TiN, (d) the EDX spectrum of STO/Cu@Ni.

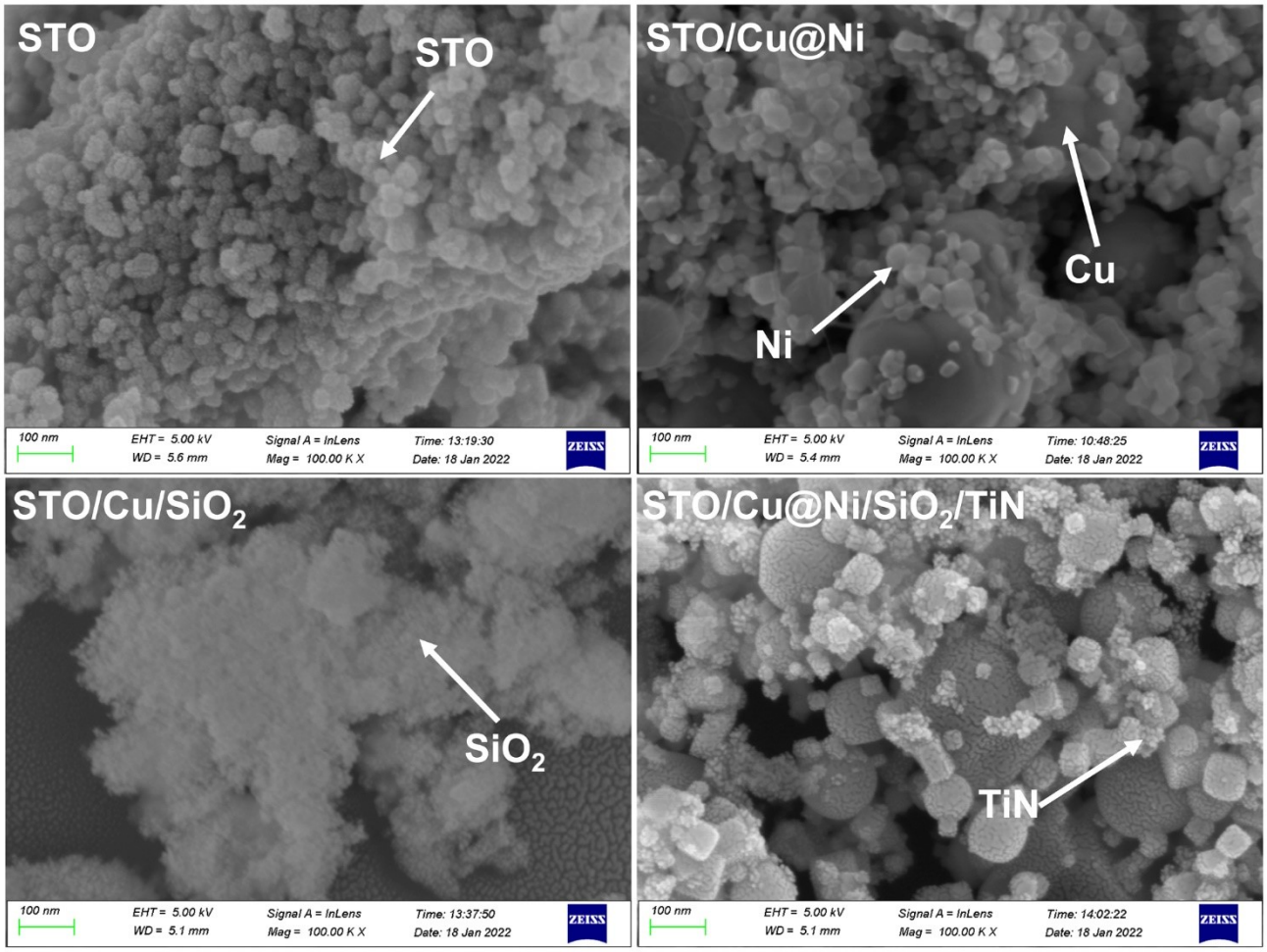

Fig. S3 the SEM images of different photocatalysts.

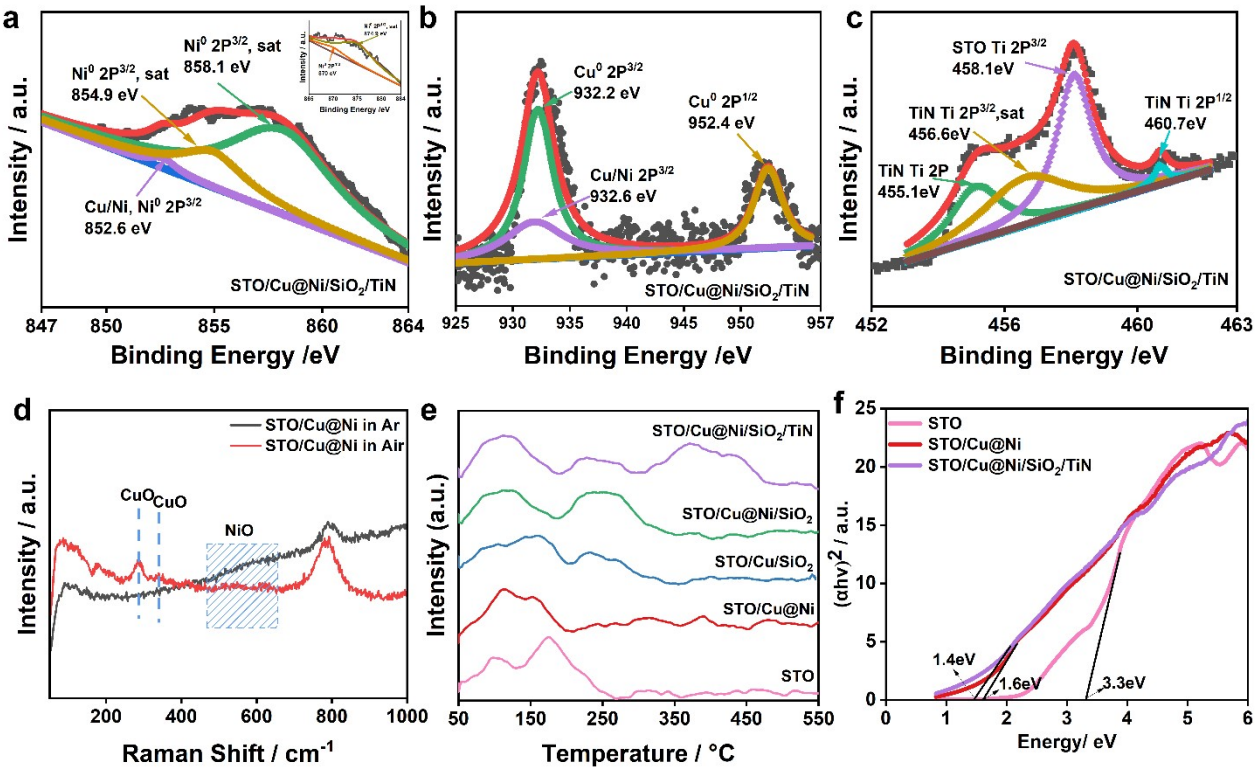

Fig. S4 (a), (b), and (c) the fitting Ni 2p, Cu 2p, and Ti 2p XPS spectra of STO/Cu@Ni/SiO_2/TiN, (d) Raman spectra of STO/Cu@Ni, (e) CO_2-TPD profiles of different photocatalysts, (f) the bandgap of STO, STO / Cu@Ni, and STO / Cu@Ni / SiO_2 / TiN.

X-ray photoelectron spectroscopy (XPS) was used to explore the surface properties of metal chemical states in STO/ Cu @ Ni/ SiO_2/ TiN photocatalysts before photocatalytic CO_2 reaction. The black dot plots represented the experimental data, while the colored lines represented the fitted lines. Fig. S4 (a) shows the characteristic peak of metallic Ni at 854.9 eV and 858.1. And the binding energy of Cu@Ni at 852.6 eV also can be found. In particular, the typical XPS spectrums of metallic Cu and Cu@Ni peaks are fitted and shown in Fig. S4 (b). Cu^0 and Cu@Ni [1] exist in the composite catalysts. The characteristic peak at 455.1eV, 456.6eV, and 460.7eV are Ti^{3+} of TiN, while the binding energy at 458.1 is Ti^{4+} of STO as shown in Fig. S4 (c). It is concluded that metallic Cu and Ni exist in the heterojunction photocatalysts. Furthermore, STO / Cu@Ni photocatalysts are measured for Raman spectra in Ar and air, respectively. There are no characteristic peaks of copper oxide and nickel oxide in Ar. However, the characteristic peaks of copper

oxide and nickel oxide appear in the air. Raman spectra also show that Cu@Ni nanoparticles exist in a metallic state as shown in Fig. S4 (d). This is important for STO/ Cu @ Ni/ SiO_2/ TiN to exhibit an excellent plasmonic effect. At the same time, the heterojunction formed between metal and semiconductor facilitates the separation of photogenerated carriers. It can be found that the CO_2-TPD profiles are that the chemisorption area of CO_2 by STO/Cu/SiO_2 increased compared with STO and STO/Cu@Ni at 250 °C - 300 °C. STO/Cu@Ni/SiO_2/TiN can still absorb CO_2 at 350 °C - 400 °C. The chemisorption area of CO_2 by STO/Cu @ Ni is slightly higher than STO/Cu.

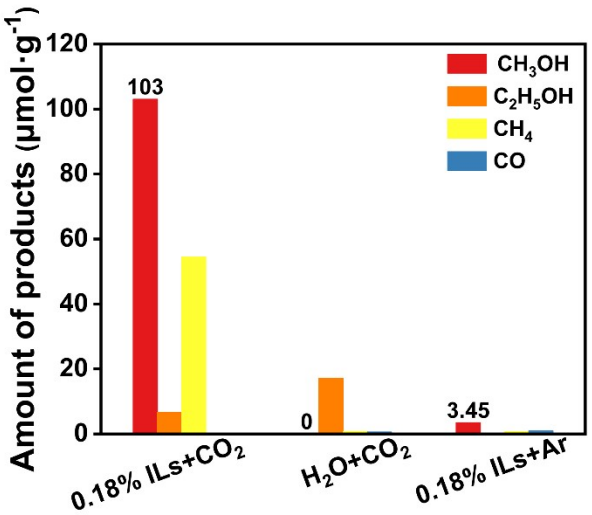

Fig. S5 products of the photocatalyst STO/Cu @ Ni/SiO_2/TiN under different reaction conditions

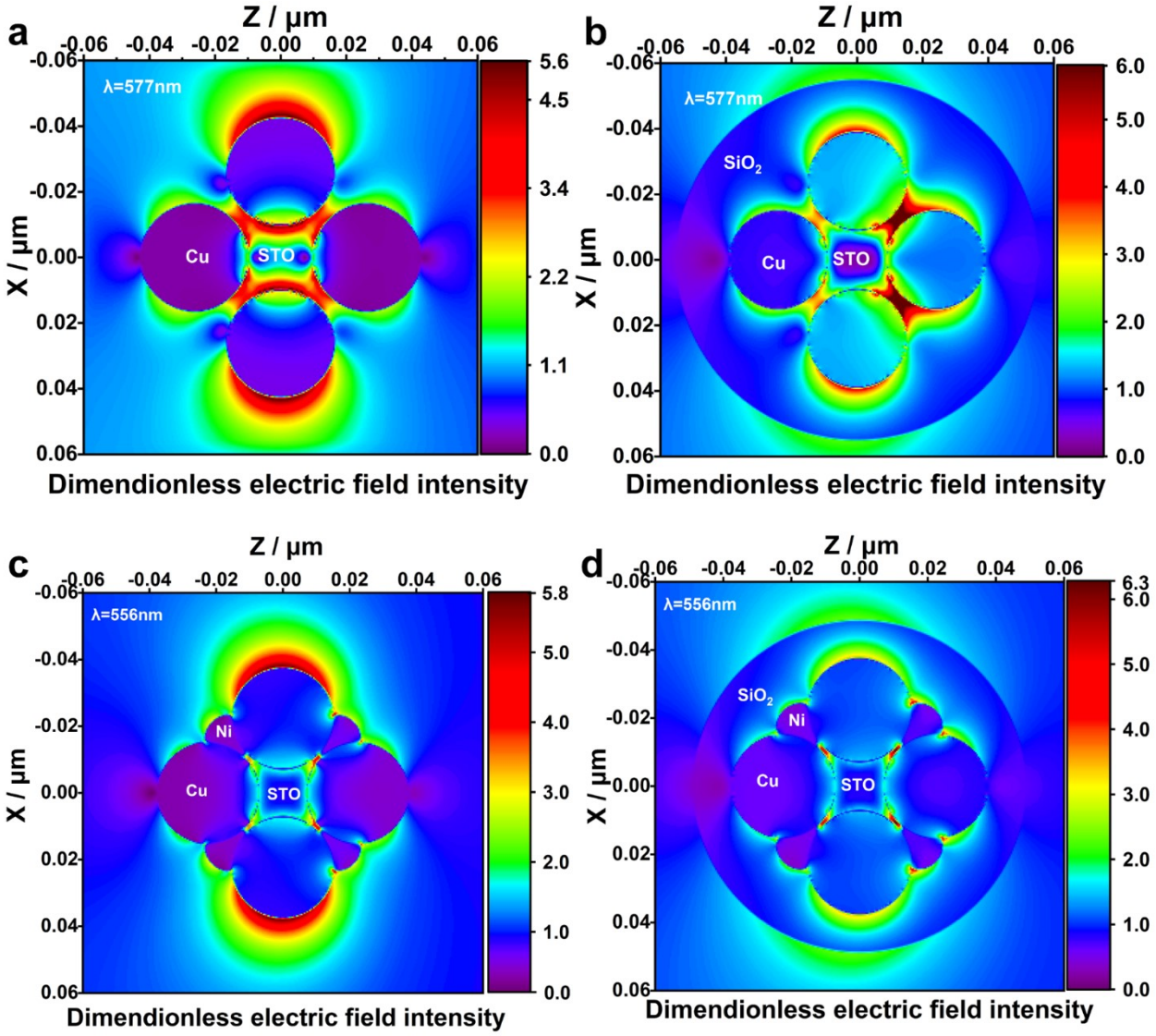

Fig. S6 (a), (b) the dimensionless electric field intensity of STO/Cu and STO/Cu/SiO_2 at the surface of Cu nanoparticles, (c), (d) the dimensionless electric field intensity of STO/Cu@Ni and STO/Cu@Ni/SiO_2 at the interface of Cu nanoparticles and Ni nanoparticles.

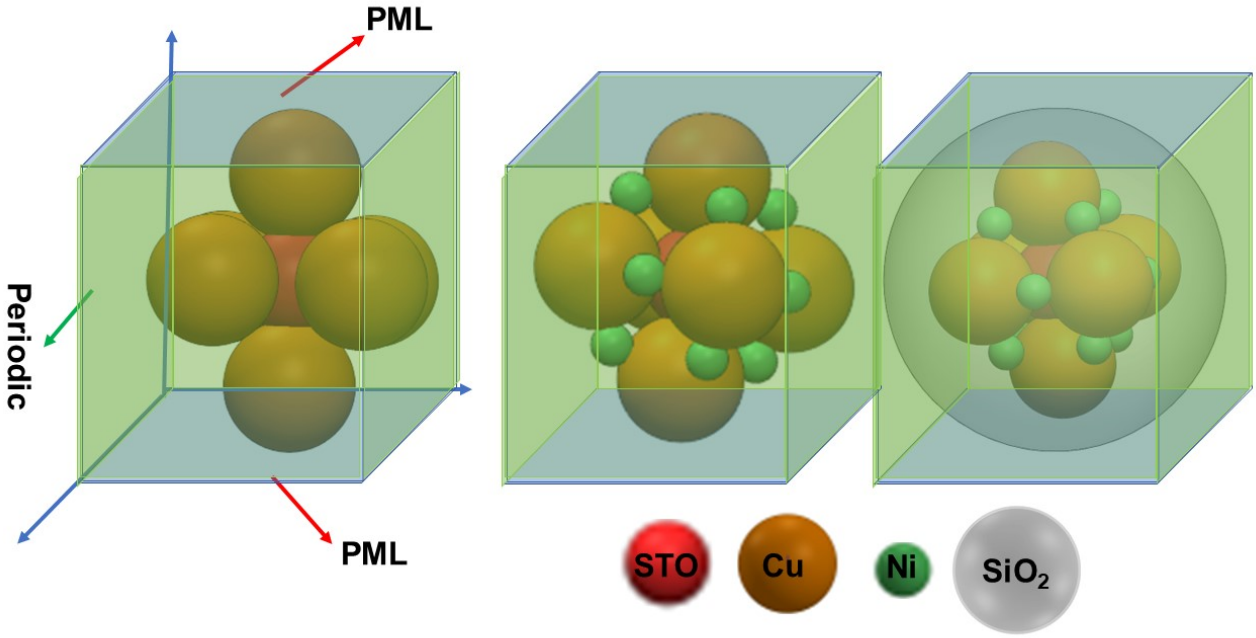

Fig. S7 FDTD model used for the composites.

Table S1 Detailed parameters used in the FDTD models.

Catalysts	FDTD model size (nm^3)
STO/Cu	300*300*500
STO/Cu@Ni	300*300*500
STO/Cu@Ni/SiO_2	300*300*500

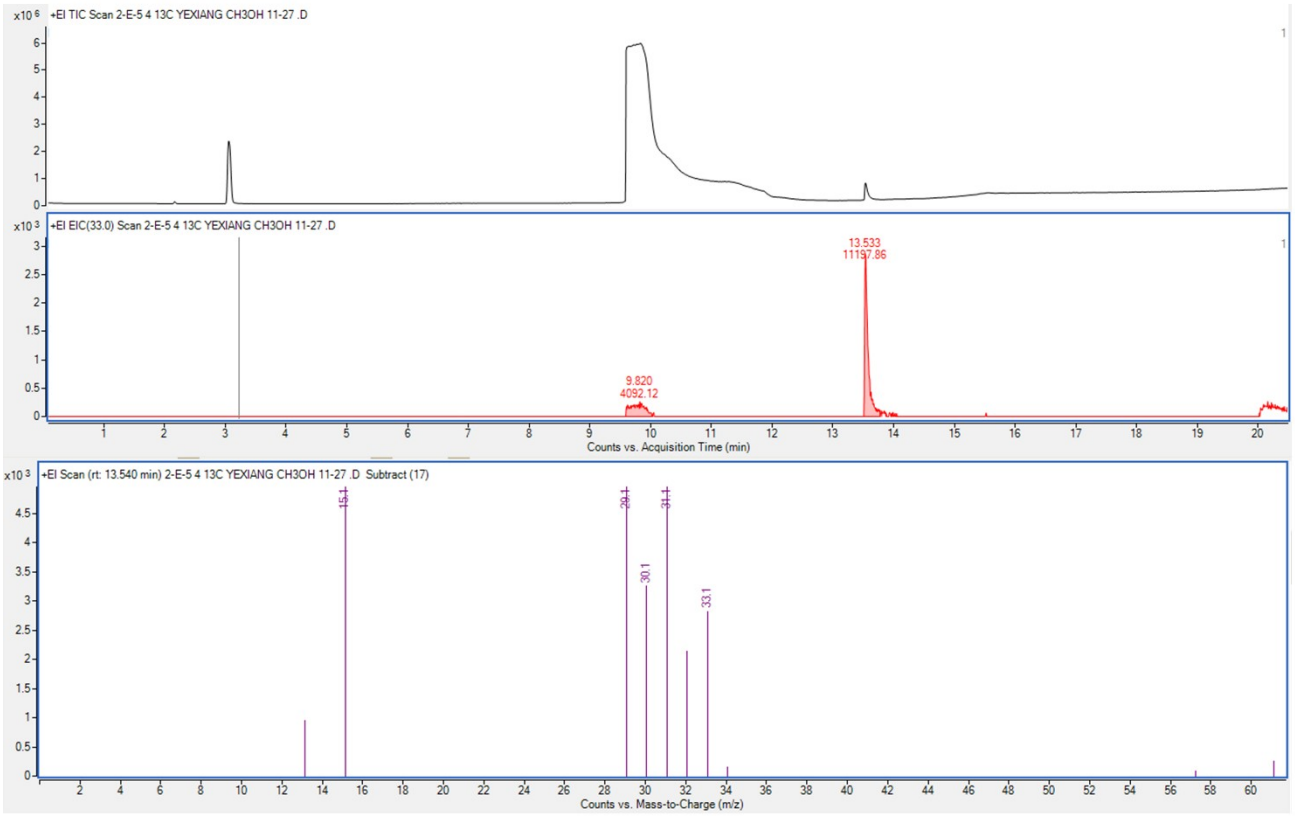

Fig. S8 the GC spectra of $^{13}CH_3OH$ (m/z=33) with $^{13}CO_2$ as carbon sources and Mass spectra of product $^{13}CH_3OH$ from the photocatalytic reaction $^{13}CO_2$ with H_2O over STO / Cu @ Ni / SiO_2 / TiN.

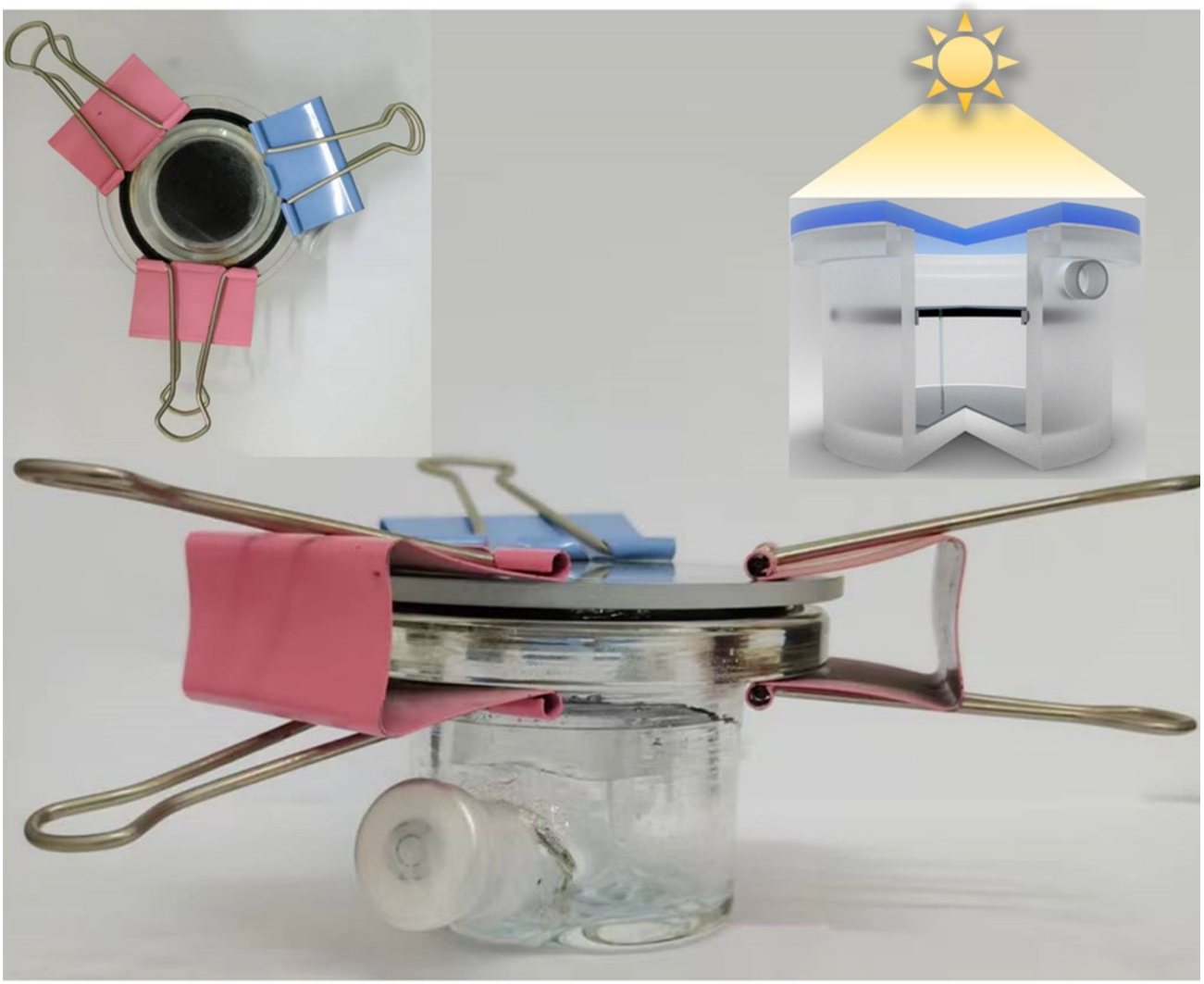

Fig. S9 Schematic diagram of reactor

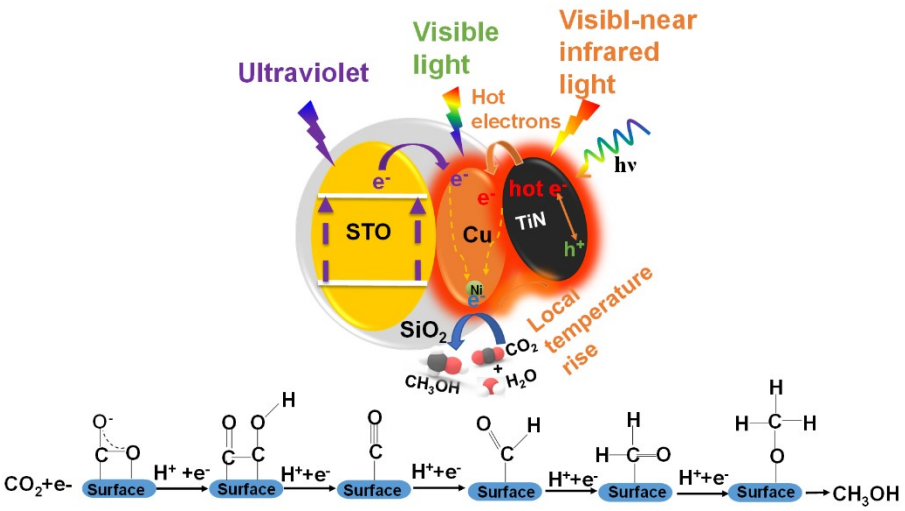

Fig. S10 the energy diagram of STO / Cu @ Ni / SiO_2 / TiN and the possible pathways for methanol.

Reference

[1] Yu, H.; Sun, C.; Xuan, Y.; Zhang, K.; Chang, K., Full solar spectrum driven plasmonic-assisted efficient photocatalytic CO_2 reduction to ethanol. Chem Engin J 2022, 430, 1-8.